Moisture sorption mechanism of aromatic polyamide fibres: diffusion of moisture into regular Kevlar as observed by time-resolved small-angle X-ray scattering technique*

Kenji Saijo, Osamu Arimoto† and Takeji Hashimoto‡
Department of Polymer Chemistry, Faculty of Engineering, Kyoto University, Kyoto 606, Japan

and Mitsuhiro Fukuda and Hiromichi Kawai
Textile Materials Science Laboratory, Department of Practical Life Studies, Hyogo University of Teacher Education, Yashiro-cho, Hyogo 673-14, Japan
(Received 22 December 1992; revised 14 May 1993)

The general trend of equatorial and meridional small-angle X-ray scattering (SAXS) was investigated for four kinds of Kevlar fibres: regular Kevlar, Kevlar 49, Kevlar 149 and a heat-treated PPTA fibre, over a scattering angle 2θ from 0.3 to 6.0°. Reflecting the fibre structure of highly oriented and extended chain conformation, the equatorial scattering is much more intensive and decreases in intensity more gradually with increasing scattering angle than the meridional scattering: i.e. the electron density fluctuations in the radial direction of the fibre due to interfibrillar and interstitial microvoids were expected to have Bragg spacings in the range from several to a few decades of angstroms, while no particular periodic fluctuation could be found in the fibre axis direction. The effects of total reflection upon the equatorial scattering intensity distribution were also discussed. The moisture sorption rate in a bone-dry regular Kevlar was observed at 25°C at saturated vapour pressure by the time-resolved SAXS technique. The experimental results were analysed assuming the moisture to be sorbed only in the microvoids to form various sizes of water cluster. Normalized moisture sorption rate, $\{1-[J(t)/J(0)]^{1/2}\}/\{1-[J(\infty)/J(0)]^{1/2}\}$, determined from the change in integrated scattering intensity over the angular range 0.3–6.0° with time, $J(t)$, was compared with that observed by a gravimetric method, $M(t)/M(\infty)$, at a relative vapour pressure of 0.896 at 25°C. Although both rate curves attained equilibrium at almost the same time of about 670 min, the rate curve from the SAXS method showed a sigmoidal shape and the moisture diffusivity was much smaller than that determined from the gravimetric method. The large discrepancy between the two diffusivities was explained using the assumption that the gravimetric method detects the sorbed water in the form of both 'micro-water clusters' and 'macro-water clusters', but the SAXS method detects only the 'macro-water clusters'.

(Keywords: sorption; small-angle X-ray scattering; Kevlar)

INTRODUCTION

The investigation of moisture diffusion and sorption in polymeric solids is a key to understanding the interaction between polymers in the solid state and water molecules, and is an important problem in practice because sorbed water molecules often cause degeneration of the physical and/or mechanical properties of the materials. Although numerous studies have been carried out on moisture sorption and diffusion in amorphous and folded-chain type semicrystalline materials[1], very few reports are available for crystalline materials with rigid and extended chain conformation, such as aromatic polyamide (aramid) fibres[2–4].

One of the aramid fibres, Kevlar®, is a typical high-tenacity and high-modulus fibre based on poly(*p*-phenylene terephthalamide) (PPTA) and developed by E.I. du Pont de Nemours & Company since 1971. In a previous paper of this series[4], we investigated the diffusion of moisture into three kinds of Kevlar fibres, regular Kevlar, Kevlar 49 and Kevlar 149, by a gravimetric method at 25°C. Since the normalized sorption curves, $M(t)/M(\infty)$ vs. $t^{1/2}$, observed for three kinds of Kevlar fibres did not obey a simple Fickian solid cylinder model except at the initial stage of the process, we analysed them using a coaxial cylinder model with the diffusion coefficients in the skin, D_{skin}, and in the core, D_{core}. For regular Kevlar and Kevlar 49, the calculated results obtained by fixing the ratio of the radius of the whole fibre to that of the core, (R_2/R_1), as 1.2, and varying

* Part XIV of the series 'Fundamental Studies on the Interaction between Moisture and Textiles' presented at the Annual Meeting of the Society of Fiber Science and Technology, Tokyo, Japan, 10 July 1990
† Present address: Chlorine Engineering Corporation Ltd, Okayama Works, 24-6 Higashi-Takasaki, Tamano-shi, Okayama 706-01, Japan
‡ To whom correspondence should be addressed

0032-3861/94/030496-08

(D_{core}/D_{skin}) from 1.5 to 7 gave a much better fit to the observed results than the solid cylinder model, over the whole range of the sorption process at various vapour pressures. The diffusion coefficients, D_{skin} and D_{core}, thus estimated were of the order 10^{-12} ($cm^2\ s^{-1}$), and 10^{-12} to 10^{-11} ($cm^2\ s^{-1}$), respectively. These results suggested, at least qualitatively, that the moisture diffusion is governed by the fibre structure, possibly by the skin–core morphology which is distinct for regular Kevlar and Kevlar 49. Our main interest in this work is, therefore, concentrated on where and how the water molecules are located in the Kevlar fibres from a more detailed morphological aspect, since the gravimetry of moisture diffusion or sorption is primarily of bulk quantity and does not give any direct information about the location of the diffused or sorbed water in the system.

Since 1975, when Yabuki *et al.*[5] estimated the diameter of microfibrils in a PPTA fibre to be about 70 Å from Hosemann plots of an equatorial wide-angle X-ray diffraction from the (2 0 0) crystal planes, several authors have suggested the existence of microfibrils and/or interfibrillar microvoids. Northolt and van Aartsen[6] reported elongated microvoids in Kevlar from small-angle X-ray scattering (SAXS). Dobb *et al.*[7] estimated the size of the microvoids in Kevlar 29 and Kevlar 49 to be several tens of angstroms in width from Guinier analysis of equatorial SAXS intensity distribution and as a few hundred angstroms in length from electron microscopy of the specimens stained by silver sulfide. Manabe *et al.*[8] also suggested microfibrils of about 100 Å in diameter by electron microscopy with a replica pattern of a freezed–crushed surface of Kevlar 49. Panar *et al.*[9] schematized the fibril of several thousand angstroms in diameter from scanning electron microscopy of HCl-etched Kevlar, although this fibril is a structural unit different from the microfibrils with which we are now dealing. Morgan and Pruneda[10] discussed the interrelationship between Na_2SO_4 impurities, microvoids and moisture sorption in Kevlar 49. Therefore, there is no doubt about the presence of microfibrils and interfibrillar microvoids, which is expected to affect the moisture diffusion and sorption of the fibres significantly.

In the present paper, we first investigate the general trend of the meridional and equatorial SAXS intensity distributions for four kinds of Kevlar fibres: regular Kevlar, Kevlar 49, Kevlar 149 and a heat-treated PPTA (HT-PPTA) fibre, and then show a new method of analysis of the diffusion of moisture into a dried regular Kevlar using a time-resolved SAXS technique based on a microvoid model. The objective here is to examine the presence of microvoids, if any, and to ascertain how the water molecules diffuse into the microvoids to make water clusters in Kevlar fibre. Two kinds of water cluster are defined in this paper. 'Micro-water cluster' refers to a bound water cluster in which several water molecules interact with the amide group by hydrogen bonds. 'Macro-water cluster' is defined as a free water cluster in which additionally sorbed water molecules interact around a 'micro-water cluster' without strong hydrogen bonds[11]. Regular Kevlar was chosen because it has the highest total moisture uptake and the fastest rate of moisture sorption among the four kinds of Kevlar fibres[4]. These two aspects are preferable for SAXS measurements because they are expected to give a bigger change in intensity distribution between the dried and moistened specimens.

EXPERIMENTAL

Multifilament yarn of the four kinds of Kevlar fibres, provided by E.I. du Pont de Nemours & Company, were washed three times in CCl_4 to remove finishing oils, if any, boiled in distilled water for 30 min and dried in air to prepare test specimens. The multifilament yarn, thus washed and air-dried, was cut into pieces several centimetres long. Forty pieces of the cut yarn were bundled so that constitutive filaments were parallel, and fixed on an X-ray sample holder 10 mm wide and 10 mm long. The bundle of test specimens thus fixed on the sample holder was further dried in a vacuum oven at 90°C for 48 h, if necessary, and moved quickly to the air-sealed sample cell of an X-ray scattering apparatus.

Figure 1 shows a schematic diagram combining the sample cell with a SAXS camera, having a maximum sample-to-detector distance of about 1 m. The camera was designed and constructed by us in 1981 using a high-flux Cu Kα beam generated from a 12 kW rotating anode type X-ray source (Rigaku Rotaflex RU-a) and a linear position-sensitive proportional counter (PSPC)[12]. The monochromatized Cu Kα beam ($\lambda = 1.54$ Å) was used with a graphite crystal and an energy discriminator in the PSPC electronics. The incident beam was collimated by a pair of pinhole slits (0.5 or 1.0 mm in diameter). In this experiment the scattered X-ray intensity distribution can be detected simultaneously by the PSPC over a range of scattering angle 2θ from 0.3 to 6.0° for the sample-to-detector distance of 47 cm. The SAXS profile was measured parallel and perpendicular to the fibre axis, called the meridional and equatorial profiles, respectively. The meridional SAXS was measured with the fibre axis parallel to the scanning direction of the one-dimensional PSPC and the equatorial SAXS with the fibre axis perpendicular to the scanning direction. The apparatus also permits a time-resolved analysis of SAXS profiles for systems undergoing relatively slow dynamic processes on a time-scale greater than ~ 1 s, such as diffusion of moisture into polymeric systems.

All the SAXS intensity profiles presented later in this paper were corrected for air-scattering and absorption.

The sample cell containing the bone-dry specimen was connected either to a vacuum pump or to a water reservoir through a valve, as shown in *Figure 1*. When the bone-dry specimen was moved into the sample cell, the cell was evacuated by the pump to keep the specimen bone-dry until the start of the moisture diffusion experiment. The sorption experiment was started by changing the valve position to connect the cell to the water reservoir in order to keep the environment of the bone-dry specimen at a constant vapour pressure of saturation. The temperature of the sample cell and water reservoir was maintained constant by a forced flow of air at about 25°C.

RESULTS AND DISCUSSION

General trend of equatorial and meridional SAXS intensity distributions from Kevlar fibres

The left- and right-hand sides of *Figure 2* show the equatorial and meridional SAXS intensity distributions, respectively, both as a function of scattering vector q ($= 4\pi \sin\theta/\lambda$) for the four kinds of Kevlar fibres under the equilibrium condition of exposure to air at about 25°C and 55% relative humidity without using the sample cell.

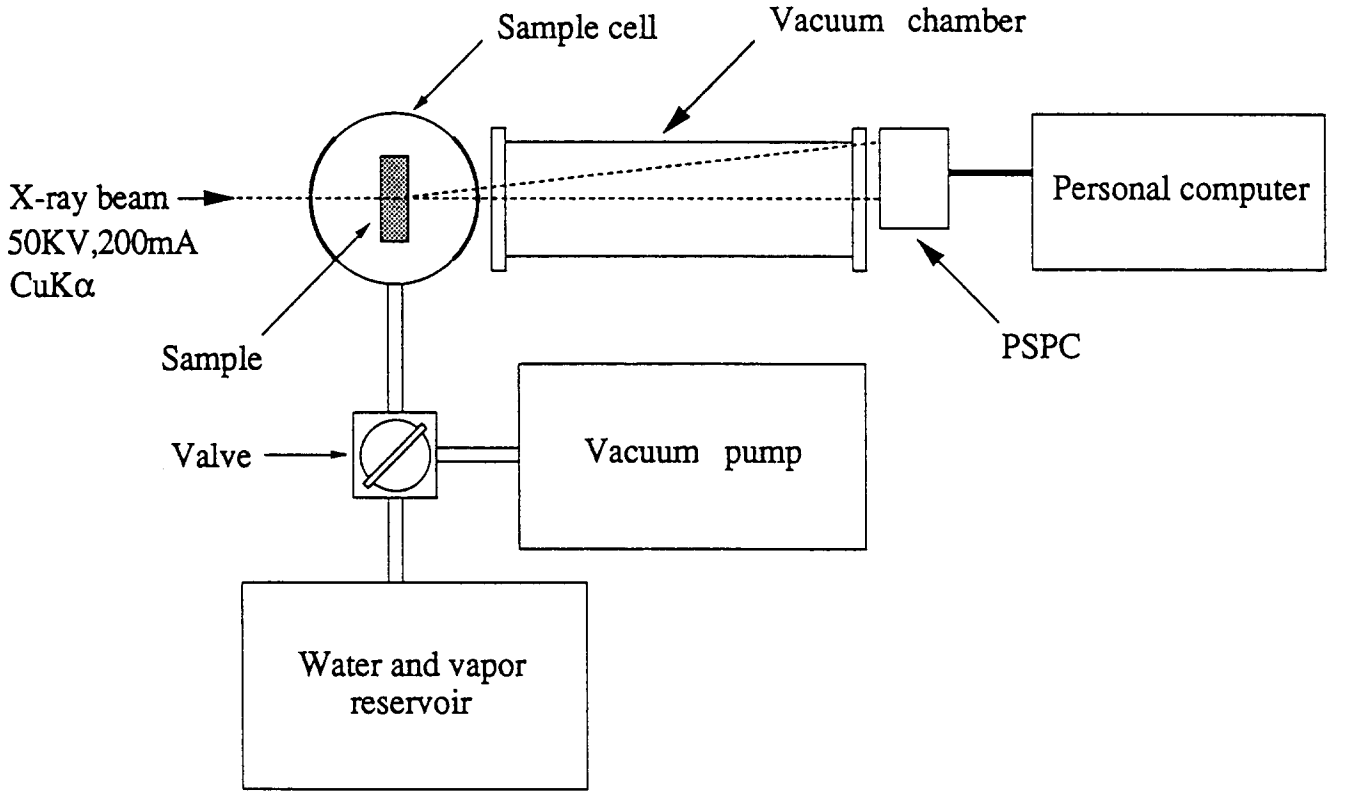

Figure 1 Schematic diagram of a SAXS apparatus combined with a sample cell, vapour pressure within the cell being kept constant

From the results in *Figure 2*, the following features may be seen:

1. The equatorial scattering is more intense than the meridional scattering for all the specimens, possibly reflecting their fibre structure.
2. A broad but definite peak with Bragg spacing of several tens of angstroms can be observed in the equatorial scattering from regular Kevlar and Kevlar 49. In the equatorial scattering from HT-PPTA and Kevlar 149, the broad peak is also observed but is not so definite.
3. Compared with ordinary polymeric systems, the equatorial scattering intensity levels of these Kevlar samples in the wide-angle range around $q = 0.2$–$0.5\ \text{Å}^{-1}$ appear to be strong and decrease gradually with increasing q. In normal polymeric systems, the intensity is weak and the intensity drop with q levels off in this q range. This excess scattering suggests the presence of interstitial microvoids in the Kevlar fibres, which exist within the fibrils and are much smaller than the interfibrillar microvoids responsible for the equatorial SAXS maximum.
4. The equatorial scattering from Kevlar 149 is considerably weaker than that from regular Kevlar, Kevlar 49 and HT-PPTA. However, the general tendency in the scattering behaviour of Kevlar 149 is the same as that in regular Kevlar, Kevlar 49 and HT-PPTA, suggesting that interstitial microvoids are present, but are fewer than in regular Kevlar, Kevlar 49 and HT-PPTA.
5. The meridional scattering from the four kinds of Kevlar fibres is not so unusual but normal in the sense that the intensity at first decreases rapidly and then levels off at the wide and tailed angular ranges with increasing q, suggesting no definite density fluctuation relevant to a long period in the fibre direction. HT-PPTA is, however, an exception, for a slight shoulder can be seen at $q \approx 0.05\ \text{Å}^{-1}$, suggesting a periodic structure along the fibre axis.

Effects of total reflection of incident X-ray beam upon SAXS intensity distribution from internal fibre structure

For an X-ray beam the refractive index of air is slightly larger than that of a polymeric material, resulting in the total reflection of an incident X-ray at their interface with a critical incident angle θ_c as small as several up to a few tens of minutes depending on the electron density of the material[13]. For PPTA the critical angle θ_c can be calculated as 10.2 minutes. The effect of the total reflection may be important at values of 2θ less than ~ 30 min for the Cu Kα radiation and can occasionally be observed in the SAXS of a bundle of fibres as an equatorial streak in the direction normal to the bundle.

Figure 3 shows a comparison of the equatorial SAXS intensity distributions between three specific samples: dried regular Kevlar kept in vacuum, dried regular Kevlar embedded in epoxy resin, and epoxy resin alone, where the instrumental conditions for these scattering measurements were kept constant. It should be pointed out that the scattering intensity distribution of Kevlar embedded in epoxy at $2\theta > 2°$ can be represented by a weighted summation of those of Kevlar and the epoxy resin. In contrast, at $2\theta < 2°$, the scattering intensity from Kevlar embedded in epoxy is lower than from Kevlar alone. (At $2\theta < 2°$, the scattering from the epoxy resin hardly contributes to the net scattering from the Kevlar embedded in epoxy; the net scattering arising almost entirely from Kevlar alone.) The intensity corrected for the volume fraction of the Kevlar fibre in the Kevlar

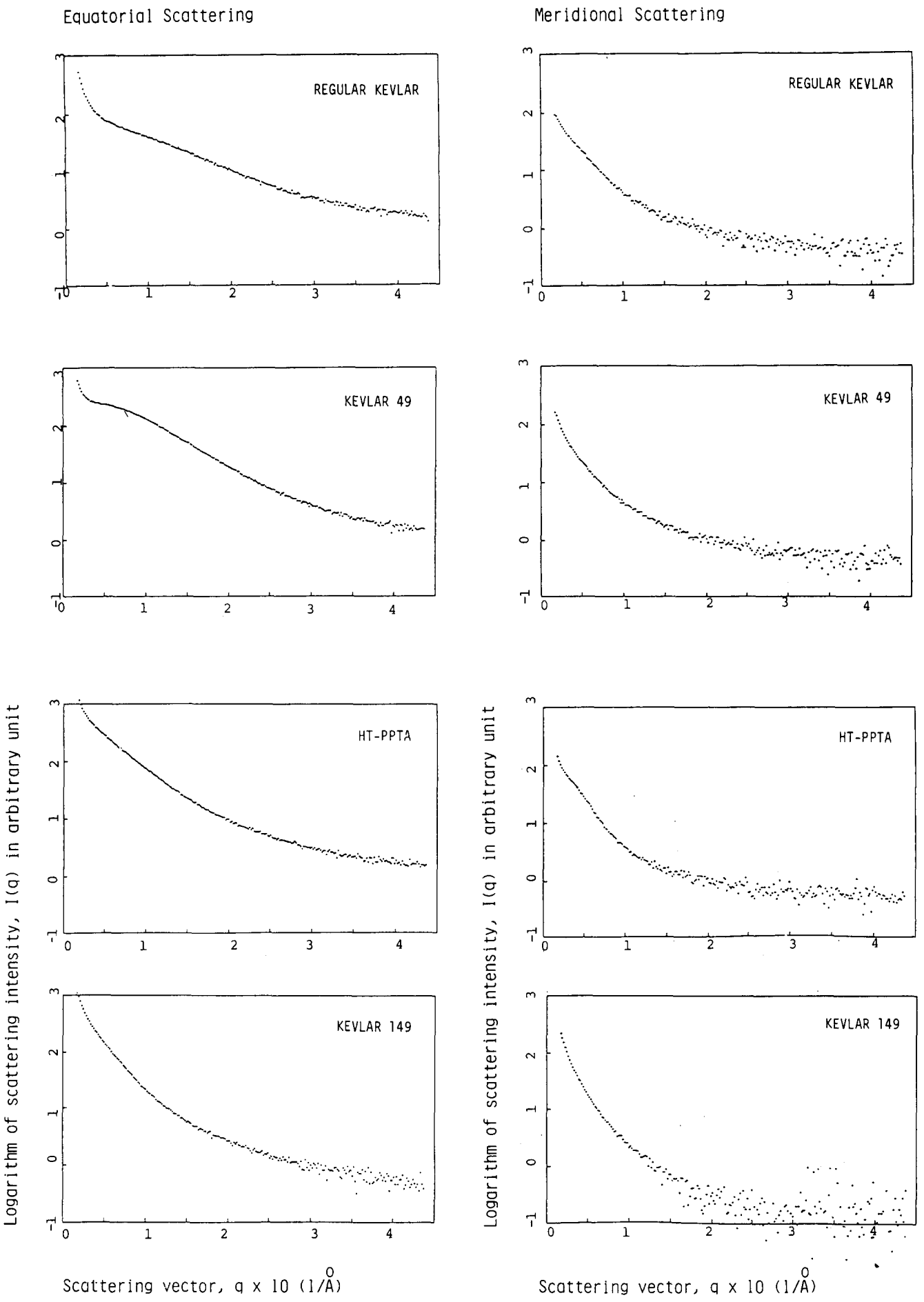

Figure 2 Equatorial (left-hand side) and meridional (right-hand side) SAXS intensity distributions as a function of scattering vector q ($=4\pi \sin\theta/\lambda$) for four kinds of Kevlar fibres under an equilibrium condition of exposure to air at about 25°C and 55% relative humidity

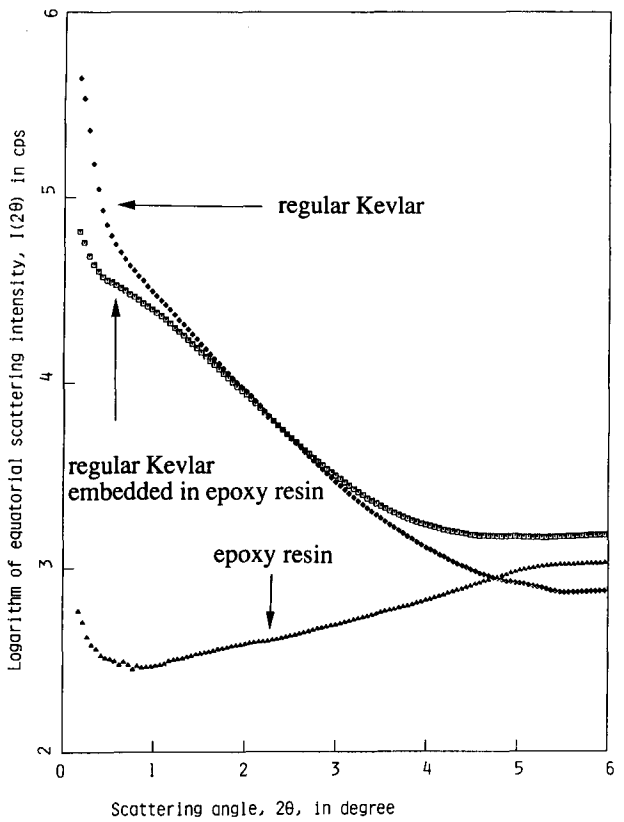

Figure 3 Comparison of equatorial SAXS intensity distribution among three specific samples: regular Kevlar (bone-dry), regular Kevlar (bone-dry and embedded in epoxy resin) and epoxy resin alone

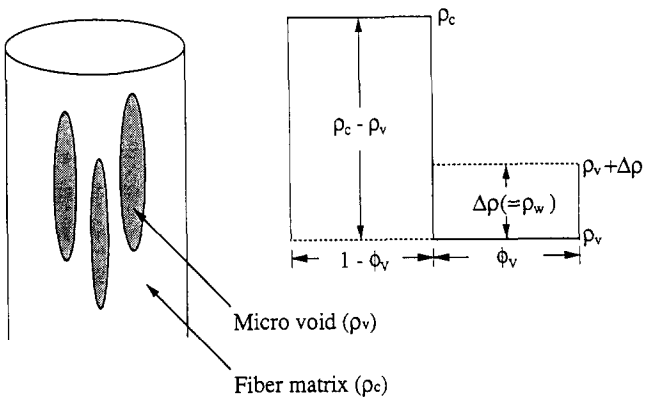

Figure 4 Two-phase model assuming the moisture to be sorbed only into microvoids dispersed within the fibre matrix. The change in electron density profile with moisture sorption is shown on the right

embedded in epoxy (~75%) is still lower than the intensity from Kevlar alone. This decrease in the SAXS intensity must be ascribed to the diminution of the effect of total reflection. Therefore, at $2\theta < 2°$, the intensity for Kevlar embedded in epoxy is essentially identical to that for Kevlar alone free from the total reflection. The reduction of the total reflection revealed more clearly a shoulder in the scattering intensity at around 1° compared with the bundle without the epoxy treatment. The shoulder can be understood as a structural characteristic associated with lateral fluctuation in electron density, possibly due to development of interfibrillar microvoids within the Kevlar fibre with a Bragg spacing of several tens of angstroms as suggested by several authors[5–10] as well as in the preceding section.

Time-resolved analysis of SAXS to determine moisture diffusivity

Let us now analyse the SAXS from the moistened fibres on the basis of a simple two-phase model, as schematized in *Figure 4*, where moisture is assumed to be sorbed only in the microvoids to form water clusters of various sizes. The change in electron density within the microvoids with time, $\rho_v(t)$, may be given by:

$$\rho_v(t) = \rho_{air}[1 - \phi_w(t)] + \rho_w \phi_w(t) \quad (1)$$

where t is the time for which the dry specimen was exposed to saturated vapour at a given temperature, ρ_{air} and ρ_w are electron densities of air and moisture, both within the void, and $\phi_w(t)$ is the volume fraction of moisture also within the void. Assuming ρ_{air} to be zero, equation (1) can be reduced to:

$$\rho_v(t) = \rho_w \phi_w(t) \quad (2)$$

The mean-square of the electron density fluctuation of the fibre specimen, $\langle \eta^2 \rangle$, can be represented by:

$$\langle \eta^2 \rangle = [\rho_c - \rho_v(t)]^2 \phi_v (1 - \phi_v) \quad (3)$$

where ρ_c is the electron density of the fibre matrix in which the voids are dispersed with volume fraction ϕ_v. Combining equation (2) with equation (3), it follows that:

$$\langle \eta^2 \rangle = [\rho_c - \rho_w \phi_w(t)]^2 \phi_v (1 - \phi_v) \quad (4)$$

At $t = 0$, equation (4) is reduced to the usual expression for two-phase systems:

$$\langle \eta^2 \rangle = \rho_c^2 \phi_v (1 - \phi_v) \quad (5)$$

The integrated scattering intensity from the fibre system, J, which is represented by:

$$J = \int_0^\infty \int_0^\infty q_1 I(q_1, q_2)\, dq_1\, dq_2 \quad (6)$$

must be proportional to $\langle \eta^2 \rangle$, where q_1 and q_2 are the scattering vectors normal and parallel to the fibre axis, respectively, and $I(q)$ is the observed scattering intensity distribution as a function of the scattering vector. The ratio of $J(t)$ to $J(0)$ can be given by that of equation (4) to equation (5), resulting in:

$$[J(t)/J(0)]^{1/2} = 1 - [\rho_w \phi_w(t)/\rho_c] \quad (7)$$

and further:

$$\rho_w \phi_w(t) = \rho_c \{1 - [J(t)/J(0)]^{1/2}\} \quad (7')$$

Here it was assumed that ϕ_v is not significantly affected by the moisture sorption, i.e. no significant structural rearrangement occurs before and after the water sorption.

As far as the present simple model is concerned, the left-hand side of equation (7') is proportional to the increment in mass of sorbed water, $M(t)$, relative to the initial dry state, and results in the following relation:

$$\frac{M(t)}{M(\infty)} = \frac{1 - [J(t)/J(0)]^{1/2}}{1 - [J(\infty)/J(0)]^{1/2}} \quad (8)$$

where $M(\infty)$ is the equilibrium mass of sorbed water at $t = \infty$. Equation (8) interrelates the change in the integrated SAXS intensity with time to a normalized diffusion rate of moisture into the voids through the matrix of fibrous material.

Although embedding the fibre bundle into the epoxy matrix is a convenient method for eliminating the effect of the total reflection on J, as demonstrated above, the

method is not necessarily adequate for the present purpose of dynamic measurement of SAXS during moisture sorption of a bundle of fibrous materials. Therefore, measurements have been performed for a bundle of regular Kevlar without embedding into epoxy resin over an angular range of 2θ from 0.3 to 6.0°. *Figure 5* shows representative results of the dynamic measurements, i.e. the change in the equatorial scattering intensity distribution of the bone-dry specimen with time of exposure to saturated vapour pressure for a time period up to 24 h (1440 min) at around 25°C. As can be seen in the figure, the scattering intensity, $I(2\theta, t)$, decreases with time particularly in an angular range of 30 to 240 minutes, possibly due to a decrease in the electron density difference between the fibre matrix and the void, as represented by equation (3).

Figure 6 shows plots of the integrated scattering intensity, $J(t)$, against the square root of time. The integrated intensity J in equation (6) was approximated by:

$$J \cong \int_{q_1'}^{q_1''} \int_{-q_2''}^{q_2''} q_1 I(q_1, q_2)\, \mathrm{d}q_1\, \mathrm{d}q_2 \qquad (6')$$

where q_1'' and q_2'' are, respectively, the upper limits of q_1 and q_2 covered in our experiment ($q_1'' = 4.4 \times 10^{-1}$ Å^{-1} and $q_2'' = 4.3 \times 10^{-2}$ Å^{-1}), above which the intensity contribution to J is not expected to be very significant (see *Figure 2*). q_1' is a minimum value of q_1 ($q_1' = 1.7 \times 10^{-2}$ Å^{-1}), above which J was calculated, and hence any structures giving rise to scattering at $q < q_1'$ were neglected in estimating J. The intensity $I(q_1, q_2)$ was measured with the linear PSPC as described earlier, with the fibre axis normal to the scanning direction of the linear PSPC, q_2''

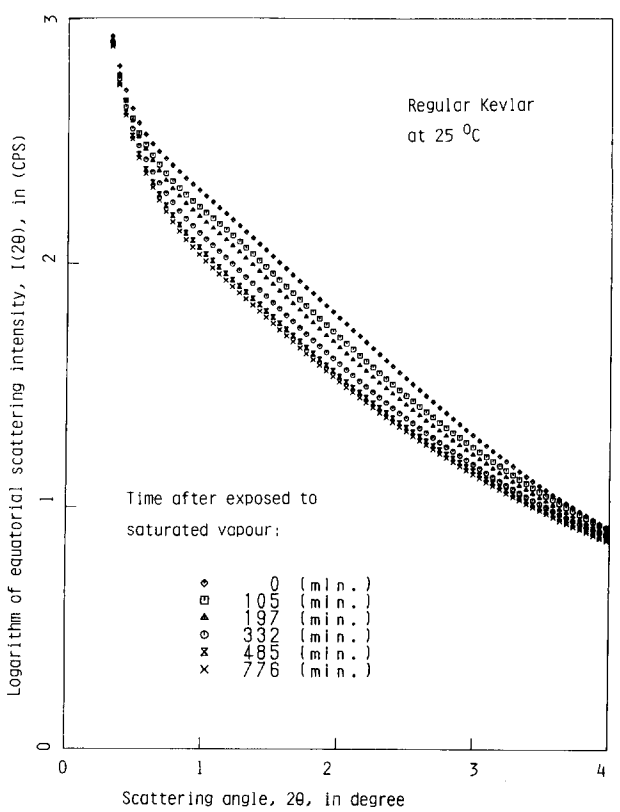

Figure 5 Change in the equatorial SAXS intensity distribution from the bone-dry regular Kevlar with time after exposing it to saturated vapour at around 25°C

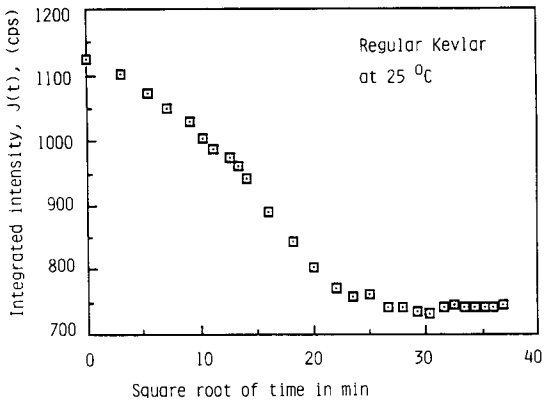

Figure 6 Change in integrated SAXS intensity from the bone-dry regular Kevlar, $J(t)$, with square root of time after exposing it to saturated vapour at around 25°C

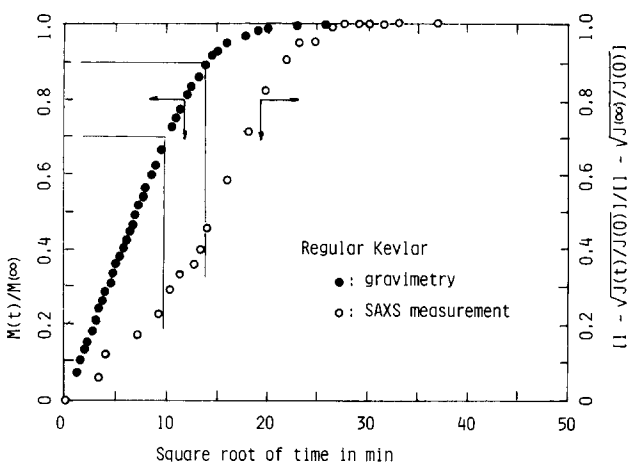

Figure 7 Plots of $\{1-[J(t)/J(0)]^{1/2}\}/\{1-[J(\infty)/J(0)]^{1/2}\}$ (○) against $t^{1/2}$, replotted from the integrated SAXS intensity, $J(t)$, in *Figure 6*, and comparison with normalized sorption rate $M(t)/M(\infty)$ determined by gravimetry (●) for the regular Kevlar at relative vapour pressure of 0.896 at 25°C (ref. 4)

being an apparent value q_2 estimated from the angle subtended by the window height of the linear PSPC (10 mm, parallel to the fibre axis) and the sample-to-detector distance. The intensity decreases with time in an inversely sigmoidal manner to level off at a time greater than ~700 min.

Comparison of the sorption rate curve determined by the time-resolved SAXS method with that by the gravimetric method

In *Figure 7*, the quantities $\{1-[J(t)/J(0)]^{1/2}\}/\{1-[J(\infty)/J(0)]^{1/2}\}$ which were recalculated from $J(t)$ in *Figure 6*, are plotted against the square root of time, exhibiting a sigmoidal increase with time to level off also at over ~700 min. In the figure, the normalized sorption rates, $M(t)/M(\infty)$, observed by a gravimetric method for the bone-dry regular Kevlar at a relative vapour pressure of 0.896 at 25°C[4], are also plotted. When the two curves are compared, we find that they both reach equilibrium at almost the same time of around 670 min.

Below about 400 min, however, there is a significant discrepancy between the two sorption rate curves, i.e. the moisture diffusivity determined from $J(t)$ at saturated vapour pressure is found to be much smaller than that determined from $M(t)$ at a relative vapour pressure of

0.896. (For this particular specimen of regular Kevlar, it was observed that the higher the vapour pressure, the larger is the moisture uptake and the faster is the attainment of equilibrium[4].)

The discrepancy between the two diffusivities, mentioned above, must be ascribed not only to the effect of the total reflection of incident X-ray, which was not eliminated by any positive means with the exception of limiting the lower integration range in equation (6) at 0.3°, but also to the simple two-phase model of moisture diffusion/sorption, as given by equations (1)–(3), on which the analysis of X-ray scattering was based. Let us first examine the effect of total reflection upon the diffusivity determined from X-ray scattering. The right-hand side of equation (8) can be rewritten as

$$\frac{1-[J(t)/J(0)]^{1/2}}{1-[J(\infty)/J(0)]^{1/2}}=\frac{J(0)^{1/2}-J(t)^{1/2}}{J(0)^{1/2}-J(\infty)^{1/2}} \tag{9}$$

If one assumes the contribution of the total reflection to the integrated scattering intensity to be given by a constant e ($J(0)\geqslant J(t)\geqslant J(\infty)>e>0$), irrespective of moisture sorption, then equation (9) can be modified to:

$$\frac{[J(0)+e]^{1/2}-[J(t)+e]^{1/2}}{[J(0)+e]^{1/2}-[J(\infty)+e]^{1/2}}\cong \frac{J(0)^{1/2}[1+(e/2J(0))]-J(t)^{1/2}[1+(e/2J(t))]}{J(0)^{1/2}[1+(e/2J(0))]-J(\infty)^{1/2}[1+(e/2J(\infty))]}$$
$$=\frac{J(0)^{1/2}-J(t)^{1/2}-(e/2)[J(t)^{-1/2}-J(0)^{-1/2}]}{J(0)^{1/2}-J(\infty)^{1/2}-(e/2)[J(\infty)^{-1/2}-J(0)^{-1/2}]} \tag{10}$$

When equation (9) is compared with the final relation in equation (10), it can be suggested that the ratio of numerator to denominator in equation (10) is always larger than that in equation (9) by a factor depending on the relative contribution of e to the integrated scattering intensity J. That is, the observed diffusivity comes out as a value larger than that of the ideal value obtained in the case in which the systems are free from total reflection, because $[J(\infty)^{-1/2}-J(0)^{-1/2}]>[J(t)^{-1/2}-J(0)^{-1/2}]\geqslant 0$. However, note that the difference between the values from equation (9) and equation (10) was found to be very small, $\leqslant 0.01$, even if we take the constant e to be as large as 300 (counts per second). It thus seems to be reasonable to neglect the effect of total reflection upon SAXS diffusivity.

At an initial stage of exposing the dry specimen to saturated vapour, moisture might be adsorbed and then condensed to form a thin water sheath on the bulk surfaces of fibrous specimens. If this is the case, it makes the gravimetric diffusivity greater to some extent than a proper value, but does not affect the diffusivity determined from SAXS. Nevertheless, the effects of the total reflection and the water sheath formation upon the moisture diffusivities seem to be too minor a factor to explain the great discrepancy between the gravimetric and the SAXS diffusivities.

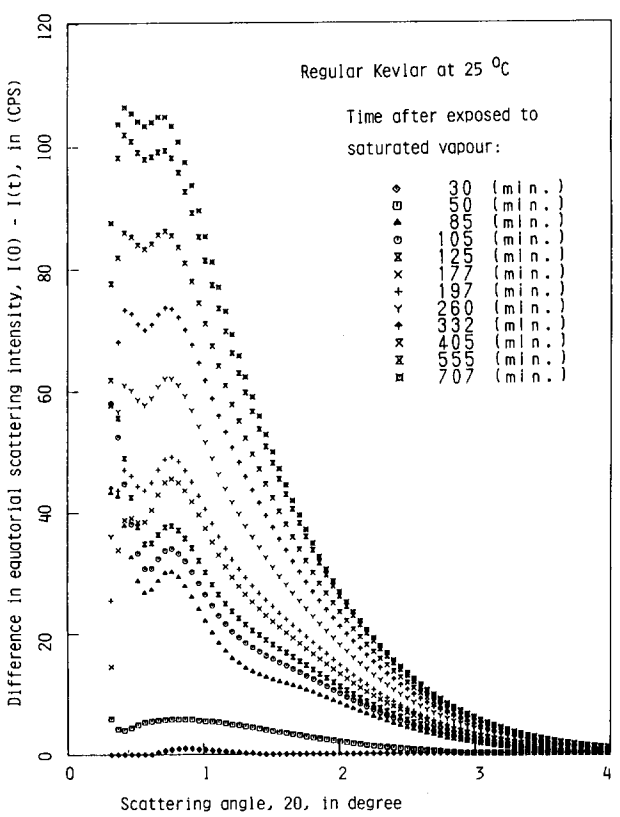

Figure 8 Change in the decrement in the SAXS intensity distribution of the bone-dry regular Kevlar with time after exposing it to saturated vapour at around 25°C

The nature of the water sorbed in regular Kevlar

We previously analysed the moisture sorption isotherm of regular Kevlar in terms of the Brunauer–Emmett–Teller (BET) multilayer adsorption model[14] by varying the number of layers, n, where the isotherm with $n=1$ corresponds to Langmuir's monolayer adsorption, those with $n_{max}\geqslant n>1$ to the BET multilayer adsorption, and those with $n>n_{max}$ to another kind of sorption mechanism such as condensation. The value of n_{max} was found to be 6–7 for this particular specimen. The amounts of the three kinds of sorbed water with $n=1$, $n_{max}\geqslant n>1$, and $n>n_{max}$ were 1.5%, 4.2% and 1.7%, respectively, in moisture regain at saturated vapour pressure.

The BET model is an extension of the Langmuir model to multilayer adsorption on assuming a type of long-range interaction between adsorbant and absorbates. It has been widely recognized that the model describes fairly well the moisture sorption isotherm of hydrophilic polymers including Kevlar fibres and distinguishes at least two categories of sorbed water: water in hydrate with $n=1$ and dissolved water with $n>1$. Existence of the water in hydrate can be simply proved by the fact that the moisture sorption of hydrophilic polymer at dryness is an exothermic process associated with substantial decreases in the hydration enthalpy and entropy of the sorbed water[3]. The nature of the dissolved water, on the other hand, has been examined by differential scanning calorimetry[15] as well as nuclear magnetic resonance[16,17] and Fourier transform infra-red spectroscopies[18,19] to designate the water in hydrate as 'loosely bound water' and 'free water' in contrast to 'tightly bound water'. It is, however, uncertain whether the free water corresponds in a quantitative manner to the sorbed water beyond $n=n_{max}$ in the BET model.

These spectroscopic examinations suggest the following picture of the build-up of two kinds of water cluster: at first the water molecule is sorbed to form a tight bond with the adsorption site with $n=1$ (monolayer adsorption); additional water molecules are bound loosely to the adsorbed water molecule to form a 'micro-water cluster' with $n_{max}\geqslant n>1$ (multilayer adsorp-

tion); and then, if space is available, the micro-water cluster grows to a 'macro-water cluster' until the space (microvoid) is filled with condensed moisture. The micro-water clusters may be too small to be detected in terms of the change in the SAXS intensity distribution within the scattering angle range adopted here, while the macro-water clusters may be localized at particular positions, such as inter- and/or intrafibrillar and interstitial microvoids and can be detected by the time-resolved SAXS technique used in this study. The moisture diffusion associated with the successive building-up of the macro-water clusters must be a slower process than the others, especially in the dense structure in the skin region[4]. This results in the smaller magnitude of the initial slope of $M(t)/M(\infty)$ vs. $t^{1/2}$ as observed by the SAXS measurements than by the gravimetric measurement, and a shift of the sorption curve by the SAXS method to longer times than by the gravimetric method. These must be the reasons for the large discrepancy between the gravimetric and SAXS diffusivities of moisture, though one of the most important structural parameters, ϕ_v, was left unresolved. In *Figure 7*, it is noteworthy that the slope of the SAXS sorption curve increases rapidly at the time when the gravimetric sorption curve attains about 70% of its normalized value and that more than half of the macro-water clusters are formed in the time interval after the gravimetric sorption curve attains 90% of its normalized value, as indicated by fine straight lines.

Differential SAXS intensity profiles free from the effects of total reflection

Finally, in *Figure 8*, we illustrate the difference in the SAXS intensity distribution between the bone-dry specimen and the moistened specimens: i.e. the change in decrement of the SAXS intensity distribution of the dried specimen with time, where the decrement is represented in terms of a linear scale of the scattering intensity. If one assumes the total reflection to be independent of moisture sorption, the decrements are free from the effects of total reflection and can be primarily ascribed to the change in electron density fluctuation with moisture sorption.

Although the data at $2\theta < 0.3°$ are very scattered, the data at $2\theta > 0.3°$ are more reliable and systematic, i.e. the decrement increases with increasing time of moisture sorption and decreases with increasing scattering angle, even showing a small but very definite peak. The peak seems to move with increasing time to a lower scattering angle, from 0.9 to 0.7° (98 Å to 126 Å in Bragg spacing), possibly due to lateral swelling of the microvoids.

ACKNOWLEDGEMENTS

The authors are deeply grateful to E.I. du Pont de Nemours & Company for providing the Kevlar fibres, and for a Scientific Research Grant to fund this study.

REFERENCES

1 Barrie, J. A. in 'Diffusion in Polymers' (Eds J. Crank and G. S. Park), Academic Press, New York, 1968, Ch. 8, p. 259
2 Penn, L. and Larsen, F. *J. Appl. Polym. Sci.* 1979, **23**, 59
3 Fukuda, M., Ochi, M., Miyagawa, M. and Kawai, H. *Text. Res. J.* 1991, **61**, 668
4 Fukuda, M. and Kawai, H. *Text. Res. J.* 1993, **63**, 185
5 Yabuki, K., Itoh, H. and Ohta, T. *Sen-i Gakkaishi* 1975, **31**, T-524
6 Northolt, M. G. and van Aartsen, J. J. *J. Polym. Sci., Polym. Symp.* 1977, **58**, 283
7 Dobb, M. G., Johnson, D. J., Majeed, A. and Saville, B. P. *Polymer* 1979, **20**, 1284
8 Manabe, S., Kajita, S. and Kamide, K. *Sen-i Kikai Gakkaishi* 1980, **33**, T-93
9 Panar, M., Avakian, P., Blume, R. C., Gardner, K. H., Gierke, T. D. and Yang, H. H. *J. Polym. Sci., Polym. Phys. Edn* 1983, **21**, 1955
10 Morgan, R. J. and Pruneda, C. O. *Polymer* 1987, **28**, 340
11 Hoeve, C. A. J. in 'Water in Polymers' (Ed. S. O. Rowland), ACS Symposium Series 127, Washington, DC, 1980, p. 135
12 Hashimoto, T., Suehiro, S., Shibayama, M., Saijo, K. and Kawai, H. *Polym. J.* 1981, **13**, 501
13 Guinier, A. 'X-ray Diffraction in Crystals and Amorphous Bodies', W. H. Freeman, San Francisco, 1963. The effect on the SAXS patterns was presented, for example, by Hashimoto, T., Nagatoshi, K., Todo, A., Hasegawa, H. and Kawai, H. *Macromolecules* 1974, **7**, 364
14 Brunauer, S., Emmett, P. H. and Teller, E. *J. Am. Chem. Soc.* 1938, **51**, 309
15 Nakamura, K., Hatakeyama, T. and Hatakeyama, H. *Text. Res. J.* 1981, **51**, 607
16 Froix, M. F. and Nelson, R. *Macromolecules* 1975, **8**, 726
17 Hatakeyama, H., Hatakeyama, T. and Nakamura, K. *J. Appl. Polym. Sci. Symp. Ser.* 1983, **37**, 979
18 Fukuda, M., Miyagawa, M., Kawai, H., Yagi, N., Kimura, O. and Ohta, T. *Polym. J.* 1987, **19**, 785
19 Fukuda, M., Kawai, H., Yagi, N., Kimura, O. and Ohta, T. *Polymer* 1990, **31**, 295